# Microstructure and Mechanical Properties of Service-Exposed HP-MA Heat-Resistant Steel Tube, Used in Cracking Furnaces

**A. Torabi [1], H. Pourmohammad *[2], A. Bahrami [3], A. Eslami [4]**

*Department of Materials Engineering, Isfahan University of Technology, Isfahan 84156-83111, Iran*

## Abstract

Cracking tubes as the main part of an olefin unit, are exposed to very harsh working conditions at both outer and inner surfaces, associated with major microstructural changes during service. Carburization, oxidation, alloying elements depletion, carbide coarsening, and secondary carbide formations are common phenomena, expected to take place in cracking tubes. This research tries to experimentally investigate the implications of cracking service exposure on microstructure and mechanical properties of the service-exposed HP-MA cracking tubes. In this regard, two tube samples after 20000 and 45000 h service at approximately 900 °C were selected. Microstructure degradation at the inner and outer surfaces of the tubes and their mid-thickness were investigated with optical and electron microscopes. By microstructural characteristics of both tube samples, it was concluded that in the 45,000-hour sample, which was more exposed to carbon, the number of secondary carbides formed on the outer surface was higher. Hardness variation across the thickness was also measured for both tubes and according to the results, in total thickness of the 45,000-hour sample, the hardness was more than the 20,000-hour specimen.

*Keywords:* Carburization, Cracking Tubes; Heat-resistant steels; HP-MA steel; Oxidation.

## 1. Introduction

Cracking furnaces are the main part of an olefin unit, in which valuable products such as ethylene are produced, through a cracking chemical reaction [1]. The heat generated to perform the thermal cracking process is radiated to the outer surface of cracking tubes in which the feed is passing by. Heat resistant cast steels are used as coils and tubes in cracking furnaces, as they have excellent high temperature corrosion resistance, oxidation resistance and high temperature creep strength [2-5]. These steels are constantly subjected to the process of decoking and on/off cycles and exposed to very harsh working conditions such as high temperatures and existence of oxidizing, nitriding and carburizing agents and atmospheres. Also, the operating temperature of these tubes varies from 800-1100 °C. [6-10]. Heat resistant cast steels are austenitic alloys, contain large amounts of carbide-forming elements in their chemical analyses, providing the room for the formation of significant amounts of uniformly distributed primary and secondary inter-dendritic carbides [11-14]. The optimal life of cracking tubes is approximately 100,000 hours if they are exposed to a temperature of 900 °C. However, it is known that oxidation and carburization reactions in cracking furnaces take place rather early, typically after 10,000 hours of operation, increasing the tubes' length and reducing their weldability [15]. This is associated with some major microstructural changes and deterioration of mechanical properties. Initially, the presence of chromium oxide layer at the surface of the tubes prevents the inter-diffusion of carbon towards the bulk of tubes.

**Corresponding author*
*Email: hodapourmohammad@ma.iut.ac.ir*
*Address: Department of Materials Engineering, Isfahan University of Technology, Isfahan 84156-83111, Iran*
*1. B.S.*
*2. M.S.*
*3. Assistant Professor*
*4. Associate Professor*

Over time, the oxide layer is damaged, resulting in the oxygen and carbon penetrations into the tubes. The diffusion of the former with high temperature oxidation, while the latter phenomenon causes carburization. Carburization is accompanied by the formation of secondary carbides and degradation of primary carbides. The effect of carburizing on the tubes can be represented by a continuous carbide network formed on the grain boundaries at elevated temperatures, which may be a favorable site for crack growth and imposes the risk of creep degradation and deterioration of ductility at high temperatures. Although some negative aspects of carburization are known, not much is known about how microstructure is evolved during carburizing service condition. This research tries to methodically investigate the implications of carburization for the microstructure and mechanical properties of service-exposed cracking tubes.

## 2. Materials and Methods

The microstructure and mechanical properties of service-exposed G4852-Micro steels, also known as HP-MA steels (which were prepared by centrifugal casting), with the thickness of 10 mm, were investigated in this study. In this regard, tube samples were taken from cracking tubes after 20000 and 45000 hours service exposure in the temperature range of 900-950 °C. Samples were cut from aged tubes to analyze the mechanical properties and to perform various tests. Chemical composition of the tube is given in Table 1.

The cross section of the samples was grounded with silicon carbide grinding papers of 80 to 1200 and then polished with 0.1 micron alumina particles. In addition, $H_2O/HF/HNO_3$ etching solution according to NACE TM0498 standard was used to prepare samples for metallographic examinations. The cross sections of the samples were also investigated by scanning electron microscope at different magnifications. Also, the inner edge, the middle region and the outer edge, were examined by chemical analysis. Vickers microhardness profilometry was carried out by applying 1 kg force on the cross section of the specimens at distances of about 1 mm from the inner to the outer surface of the tube.

## 3. Results and discussion

Fig. 1 shows microstructure of the as-cast heat-resistant specimen, before service exposure. In the image taken from the cross section of the sample, austenitic background and primary skeletal $M_{23}C_6$ carbides at grain boundaries, where M comprises Fe and Cr, can be seen.

Fig. 2 depicts EDS analyses of different phases in the as-cast specimen. The white phase in this structure is rich in Nb, which can be concluded it is a niobium carbide phase. The grayish phase, on the other hand, is rich in chromium, inferring that this phase is a chromium carbide phase.

Table 1. Chemical composition of the investigated tube.

| Sample | C | Ni | Cr | P | S | Si | Mn | Mo | Nb | Ti |
|---|---|---|---|---|---|---|---|---|---|---|
| **Service-Exposed Tube** | 0.4 | 35.0 | 26.3 | 0.015 | 0.01 | 0.9 | 1.0 | 0.1 | 0.9 | 0.008 |
| **ASTM A 608-20** | 0.38 –0.45 | 34.0 – 37.0 | 24.0 – 27.0 | 0.03 max | 0.03 max | 0.50 – 1.50 | 0.50 –1.50 | 0.50 max | 0.50 –1.50 | - |

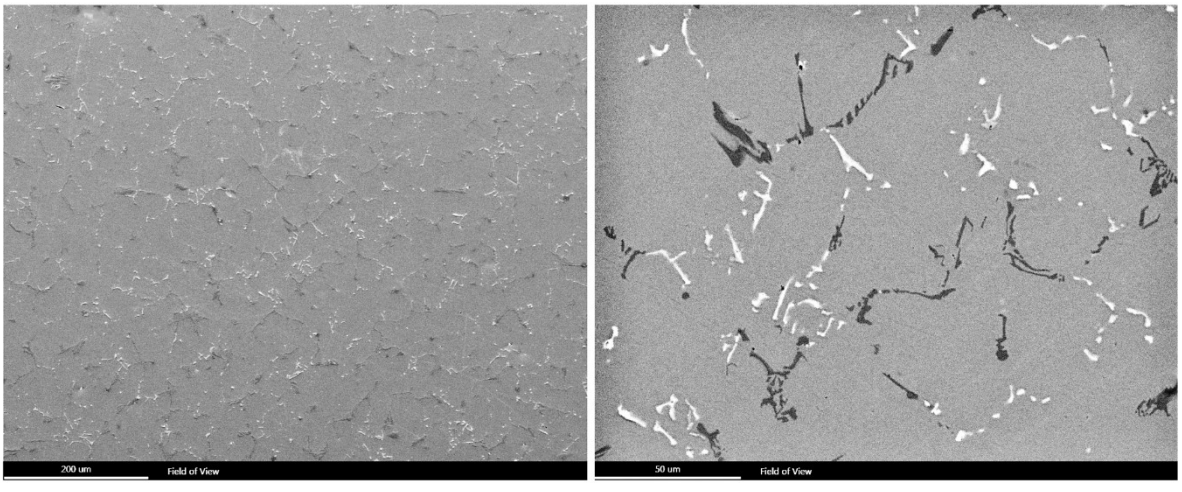


Fig. 1. Typical SEM micrograph of as-cast HP-MA alloy.

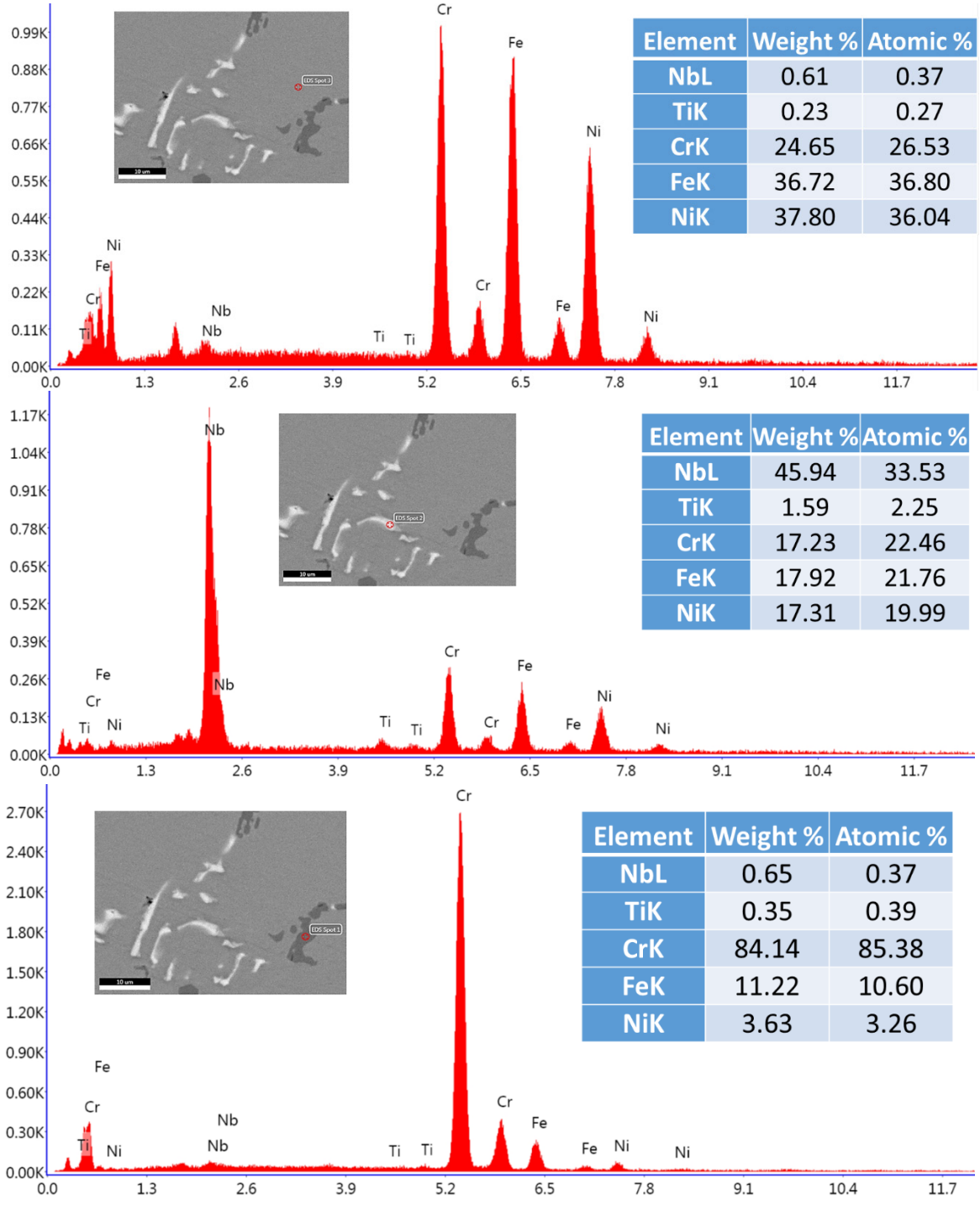


Fig. 2. EDS analyses of different phases: the matrix, the white phase and the grayish phase in the as-cast structure.

Figs. 3 to 7 show microstructures and EDS chemical analyses of different phases at the inner, the middle and the outer surfaces of aged tubes after 20000 and 45000 hours of service exposure, which are shown from the outer surface towards the inner surface, respectively. As can be seen, both the inner and outer surfaces are heavily influenced by the service exposure, with the thickness of influenced surface layer being larger for the 45000 hours service exposed specimen. The influenced surface layer at both sides contains large blocky shaped islands of black/grayish phases. Moreover, the surface layer appears to be lean in carbide phases. One can also notice that moving towards the outer surfaces, number of fine secondary carbide particles ($M_7C_3$ and $M_{23}C_6$ secondary carbides) increases. It is known that the outer surface is more exposed to carbon, resulting in the penetration and diffusion of carbon towards the bulk of the tube. This, in turn, is associated with the conversion of primary

$M_{23}C_6$ carbides to $M_7C_3$ carbides and formation of newly-formed fine carbide particles [15].

Figs. 5 and 6 depicts SEM micrographs of aged samples, after 20000 and 45000 hours of service. Again, these micrographs show how the structure at both inner/outer surfaces are degraded. In fact, the protective layer of chromium oxide ($Cr_2O_3$) on the surface is an extremely important feature of this alloy, as it prevents the penetration of oxygen and carbon and other harmful elements towards the bulk structure. It appears that service exposure has severely degraded the mentioned protective layer, meaning that the surface structure can no longer resist the penetration of carbon. The fact that Si-rich oxide phases (black phases, see Fig. 7a) have been formed is an indication that the surface and internal oxidation reactions have become active at the early stage of service and operations. EDS results show that while Si-rich oxides are more formed further away from the surface, Cr-rich oxide phases (grayish phase, see Fig. 7b) are observed as a rather thick and porous layer at the surface. This possibly has to do with the difference in the diffusion rates of Cr and Si. This mentioned service-originated Cr-rich oxide layer is typically very porous and in some areas it is further developed to the bulk of the alloy. As a result, the diffusion of carbon into the structure becomes easier, resulting in the carbide coarsening and formation of secondary carbides. The former phenomenon leads to a decrease in high temperature mechanical properties, more specifically creep resistance. The penetration of carbon into the substrate is associated with carburization, and therefore matrix hardening. In order to regenerate the degraded $Cr_2O_3$ layer, the existing chromium in the matrix diffuses towards the surface, resulting in the formation of Cr-depleted areas near the surface. On the other hand, inside the tubes, there is oxygen that has penetrated into the structure and formed dark oxides, which are shown in the inner surface images of the samples. For the sample with 20000 hours service life, this surface layer has a thickness of 250 µm, while in sample with 45000 hours service life, this thickness has increased to 450 µm.

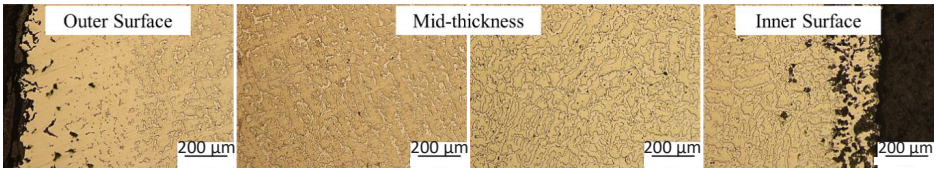


Fig. 3. Typical optical microscope images of the sample after 20,000 hours of service.

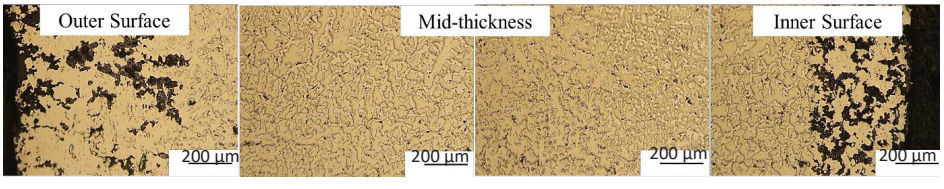


Fig. 4. Typical optical microscope images of the sample used after 45,000 hours of service.

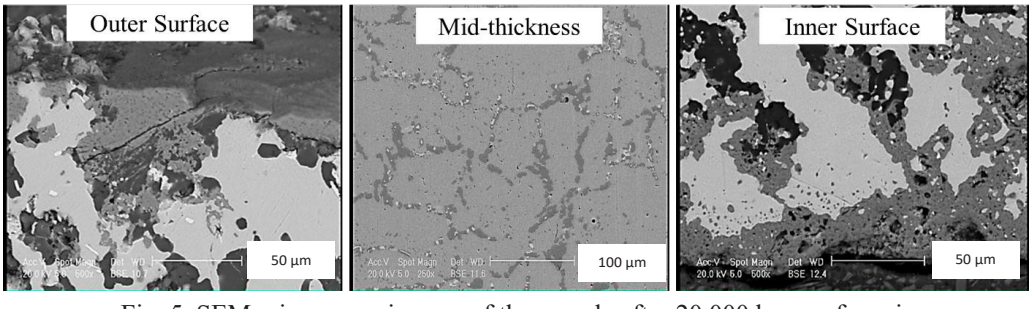


Fig. 5. SEM microscope images of the sample after 20,000 hours of service.

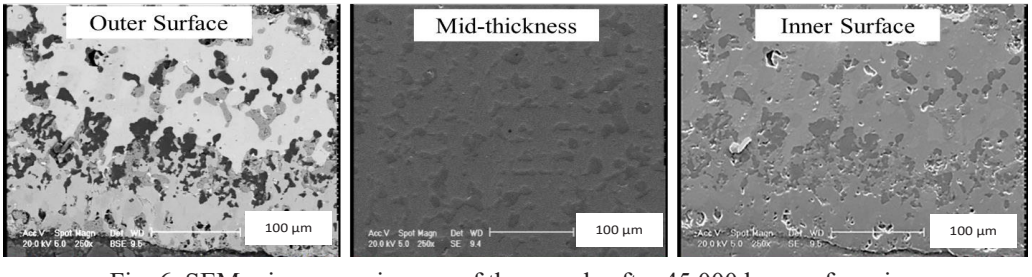


Fig. 6. SEM microscope images of the sample after 45,000 hours of service.

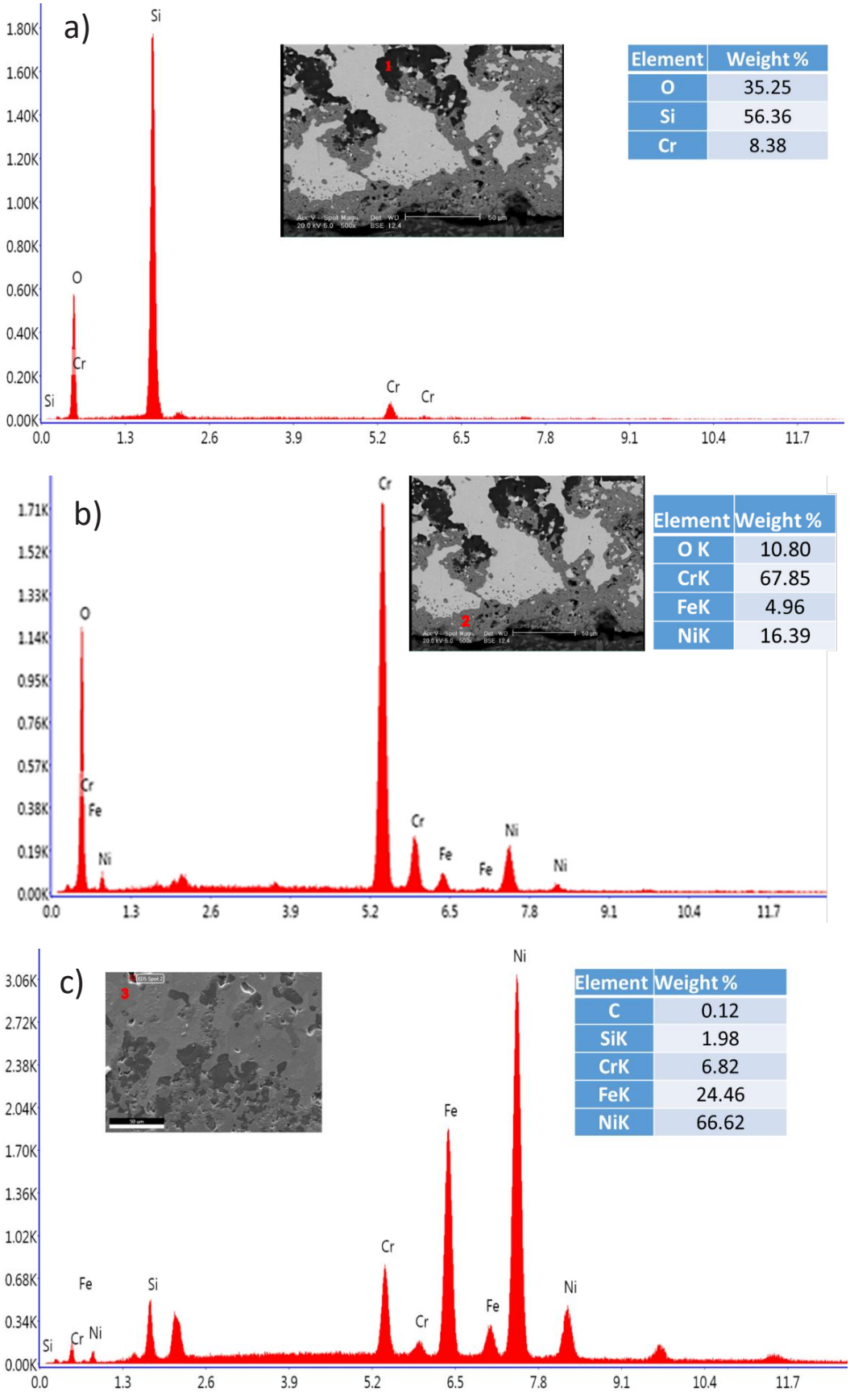


Fig. 7. EDS analyses of a) black phase, b) grayish phase, and c) the matrix in aged samples.

Fig. 8 depicts macro images of the cross-section of the tube after 20000 and 45000 hours of service. The color difference is attributable to the carburized layer. The lighter area is the carburized layer. Fig. 8 shows that the higher the ageing time, this thicker is the carburized layer is, such a way that in 45000-hour aged specimen, almost 70% of the total thickness is carburized.

Figs. 9 and 10 depict elemental mapping at the inner and outer surfaces of the 20000-hour aged specimen, respectively. It appears that both the inner and the outer surfaces are heavily influenced by oxygen, as a thick oxygen layer is seen at both surfaces. Also, it is seen that the segregation of Mn and Cr towards the surface is more pronounced at the outer surface, which has to do with more aggressive environment at the outer side of tubes. A heavily depleted Cr/Mn zone is also visible at the outer surface of the tubes. Another noticeable difference between the outer and the inner surface of the tubes, is morphology of silicon oxide phase. A distribution of rather fine globular silicon oxide particles are observed at the outer surface of tubes, while that is not seen in the inner surface.

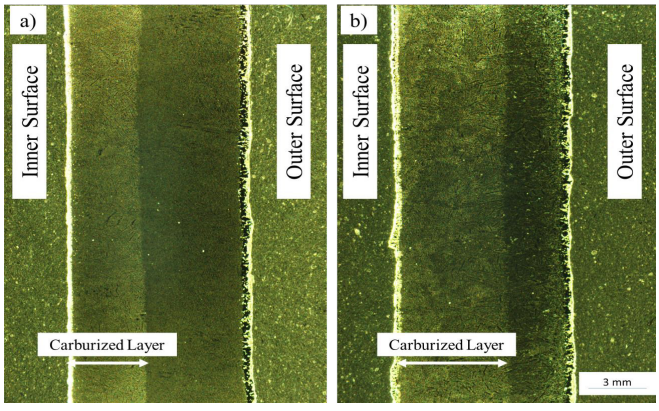


Fig. 8. Macro images of aged tubes, after a) 20000 hours and b) 45000 hours of service exposure.

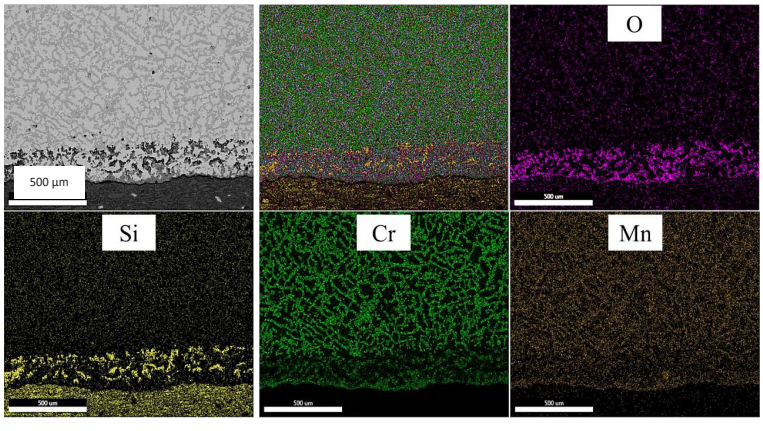


Fig. 9. Elemental mapping at the inner surface of the 20000-hours aged tube sample.

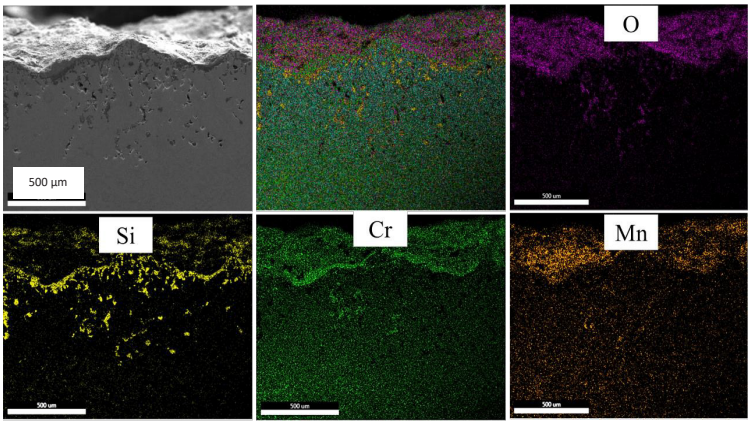


Fig. 10. Elemental mapping at the outer surface of the 20000-hours aged tube sample.

Figs. 11 and 12 depict elemental mapping at the inner and outer surfaces of the 45000-hour aged tube specimen, respectively. It is seen that longer service exposure from 20000 to 45000 hours is associated with the extension of surface-influenced layer. For example, the thickness of oxygen-rich layer at the inner surface has increased to values over 1000 µm after 45000 hours of service, while that in the 20000 hours exposed tube is roughly 200 µm. A comparatively more extensive Cr/Mn-segregated and depleted zones are also noticeable in this sample.

The formation of oxides at the inner/outer surfaces of tube samples, leads to the depletion of elements such as chromium and silicon compared to the middle thickness, which causes a decrease in oxidation resistance, while in the middle thickness, these oxide phases are rarely formed. In addition, because the inner surface of the tube is more exposed to carburizing gases, chromium, in particular, has a strong tendency to react with carbon and secondary carbides are formed in the structure. Due to the presence of oxygen in the furnace atmosphere, it can easily penetrate into the surface of the tubes and oxide phases are formed on the outer surfaces. Since around these oxide phases, it is a suitable place for formation of micro cracks, and network and continuous carbides have changed to separated carbides at a microscopic scale, according to the images, it can be concluded that oxide particles at the surface are preferential sites for the nucleation of micro-cracks. An example of a micro-crack, formed at the end of an oxide island is represented in Fig. 13. The micro-crack in this case is roughly 200 µm.

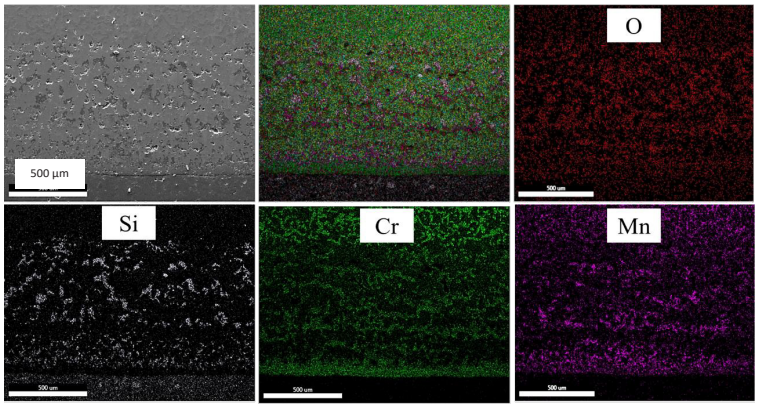


Fig. 11. Elemental mapping at the inner surface of the 45000 hours aged tube sample.

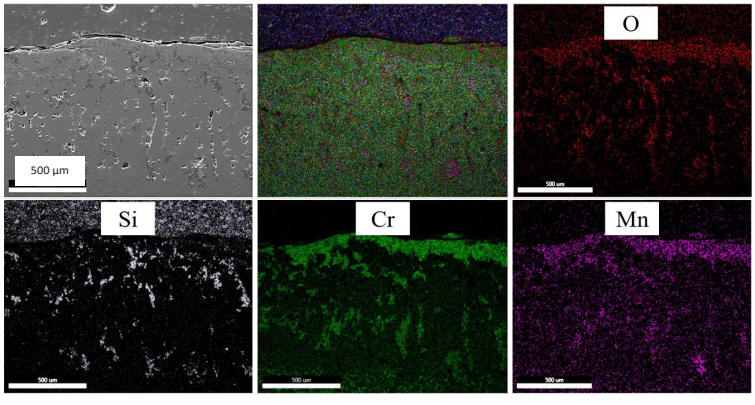


Fig. 12. Elemental mapping at the outer surface of the 45000 hours aged tube sample.

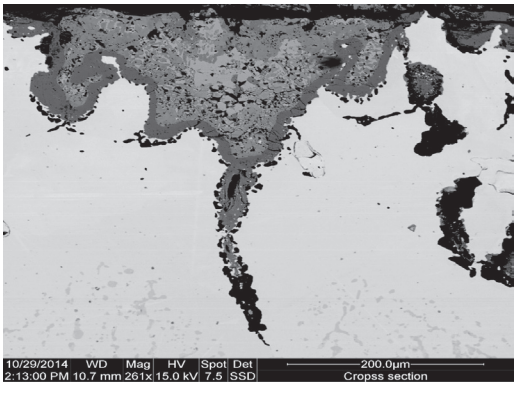


Fig. 13. Micro-cracks, formed at the inner surface of service-exposed tube.

Vickers microhardness measurements for sample with 45000 hours of service, and sample for 20000 hours of service are shown in the Fig. 14. By comparing the presented data, it is concluded that the sample with 45000 hours of service has higher hardness than the sample with 20000 hours of service because it had been exposed to carburization and oxidation for a longer period, associated with the formation of secondary carbides in the structure. According to this diagram, for the 45000 hours service-exposed tube, the hardness is significantly reduced in chromium-depleted areas. However, moving towards the middle thickness of the sample, the hardness gradually increases. 20000 hours service-exposed tube has less hardness changes through the thickness due to lower service time. With mentioning to say that, hardness differences through the thickness can be deleterious when it comes to thermal shock resistance.

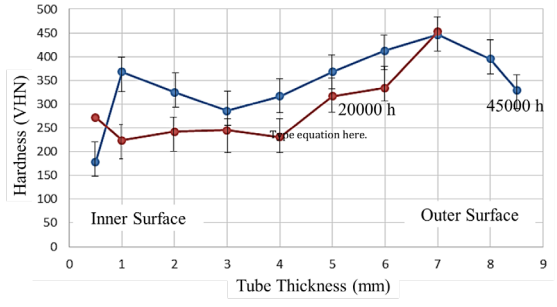


Fig. 14. Microhardness of the tubes from inner surface towards the outer surface.

## Summary

According to this study, it can be concluded that the causes of degradation of alloy steel used in ethylene cracking tubes in petrochemical industry was severe carburization and oxidation. Two tube samples were examined in this investigation: one with service exposure of 20,000 hours and the other after 45,000 hours of service. The investigated tubes had several microstructural characteristics. In this regard, the inner and outer surfaces of the investigated tube samples were exposed to severe oxidation and depletion of chromium and manganese. In addition, carbide particles for the 45,000 hours aged sample were coarser in appearance. Eventually, these continuous and lattice carbides were dispersed, forming suitable locations for initiation of micro cracks; and cracks are expected to form in the samples. As these micro cracks grow, the tube could eventually fail.

## Acknowledgment

The authors would like to thank Isfahan University of Technology for its support.

## References

[1] L.H. Almedia, A.F. Ribeiro, I. Le May, Microstructural characterization of modified 25Cr–35Ni centrifugally cast steel furnace tubes. Materials Characterization, 49(3), pp.219-229.
[2] C.J. Liu, Y. Chen, Variations of the microstructure and mechanical properties of HP40Nb hydrogen reformer tube with time at elevated temperature. Materials & Design, 32(4), pp.2507-2512.
[3] N. Roy, A. Raj, B.N. Roy, A.K. Ray, Creep deformation and damage evaluation of service exposed reformer tube. Canadian metallurgical quarterly, 54(2), pp.205-222.
[4] A.R. Andrade, L.H.C. Bonazzi, Influence of niobium addition on the high temperature mechanical properties of a centrifugally cast HP alloy. Materials Science and Engineering: A, 628, pp.176-180.
[5] S. Shi, J.C. Lippold, Microstructure evolution during service exposure of two cast, heat-resisting stainless steels—HP–Nb modified and 20–32Nb. Materials Characterization, 59(8), pp.1029-1040.
[6] R. Viswanathan, An Overview of Failure Mechanisms in High Temperature Components in Power Plants. Electric Power Research Institute, 122, 246-255.
[7] A. Goswami, S. Kumar. Failure of pyrolysis coils coated with anti-coking film in an ethylene cracking plant. Engineering Failure Analysis, 39, pp. 181-187.
[8] F.C. Nunes, L.H. de Almeida, J. Dille, J.L. Delplancke, I. Le May, Microstructural changes caused by yttrium addition to NbTi-modified centrifugally cast HP-type stainless steels. Materials Characterization, 58(2), pp.132-142.
[9] M. Santos, M. Guedes, R. Baptista, V. Infante, R.A. Cláudio. Effect of severe operation conditions on the degradation state of radiant coils in pyrolysis furnaces. Engineering Failure Analysis, 56, pp. 194-203.
[10] J. Yan, Y. Gao, F. Yang, C. Yao, Z. Ye, D. Yi, S. Ma, Effect of tungsten on the microstructure evolution and mechanical properties of yttrium modified HP40Nb alloy. Materials Science and Engineering: A, 529, pp.361-369..
[11] J.M. Yu, V.H. Dao, V. Lok, T.G. Le, K.B. Yoon, Asymptotic creep deformation behavior of modified HP steel after long-term service. Journal of Mechanical Science and Technology, 34(5), pp.1997-2009.
[12] A. Bahrami, P. Taheri, Creep failure of reformer tubes in a petrochemical plant. Metals, 9(10), p.1026.
[13] C. Maharaj, A. Marquez, R. Khan, Failure analysis of Incoloy 800HT and HP-modified alloy materials in a reformer. Journal of Failure Analysis and Prevention, 19(2), pp.291-300.
[14] A.C. McLeod, C.M. Bishop, K.J. Stevens, M.V. Kral, Microstructure and carburization detection in HP alloy pyrolysis tubes. Metallography, Microstructure, and Analysis, 4(4), pp.273-285.
[15] H. Pourmohammad, A. Bahrami, A. Eslami, M. Taghipour, Failure investigation on a radiant tube in an ethylene cracking unit. Engineering Failure Analysis, 104, pp.216-226.